Open access • Posted Content • DOI:10.1101/2021.05.04.442663

SARS-CoV-2 variant B.1.617 is resistant to Bamlanivimab and evades antibodies induced by infection and vaccination — Source link

Markus Hoffmann, Markus Hoffmann, Heike Hofmann-Winkler, Nadine Krueger ...+15 more authors

Institutions: German Primate Center, University of Göttingen, University of Erlangen-Nuremberg, Hannover Medical School

Published on: 05 May 2021 - bioRxiv (Cold Spring Harbor Laboratory)

Topics: Antibody

SARS-CoV-2 variant B.1.617 is resistant to Bamlanivimab and evades antibodies induced by infection and vaccination

Markus Hoffmann,[1,2,6,*] Heike Hofmann-Winkler,[1,6] Nadine Krüger,[1,6] Amy Kempf,[1,2] Inga Nehlmeier,[1] Luise Graichen,[1,2] Anzhalika Sidarovich,[1,2] Anna-Sophie Moldenhauer,[1] Martin S. Winkler,[3] Sebastian Schulz,[4] Hans-Martin Jäck,[4] Metodi V. Stankov,[5] Georg M. N. Behrens,[5] Stefan Pöhlmann[1,2,*]

[1]Infection Biology Unit, German Primate Center, Kellnerweg 4, 37077 Göttingen, Germany

[2]Faculty of Biology and Psychology, Georg-August-University Göttingen, Wilhelmsplatz 1, 37073 Göttingen, Germany

[3]Department of Anaesthesiology, University of Göttingen Medical Center, Göttingen, Georg-August University of Göttingen, Robert-Koch-Straße 40, 37075 Göttingen, Germany

[4] Division of Molecular Immunology, Department of Internal Medicine 3, Friedrich-Alexander University of Erlangen-Nürnberg, Glückstraße 6, 91054 Erlangen, Germany

[5] Department for Rheumatology and Immunology, Hannover Medical School, Carl-Neuberg-Str. 1, 30625 Hannover, Germany

[6]These authors contributed equally

[7]Lead contact

*Correspondence: mhoffmann@dpz.eu (M.H.), spoehlmann@dpz.eu (S.P.)

SUMMARY

The emergence of SARS-CoV-2 variants threatens efforts to contain the COVID-19 pandemic. The number of COVID-19 cases and deaths in India has risen steeply in recent weeks and a novel SARS-CoV-2 variant, B.1.617, is believed to be responsible for many of these cases. The spike protein of B.1.617 harbors two mutations in the receptor binding domain, which interacts with the ACE2 receptor and constitutes the main target of neutralizing antibodies. Therefore, we analyzed whether B.1.617 is more adept in entering cells and/or evades antibody responses. B.1.617 entered two out of eight cell lines tested with slightly increased efficiency and was blocked by entry inhibitors. In contrast, B.1.617 was resistant against Bamlanivimab, an antibody used for COVID-19 treatment. Finally, B.1.617 evaded antibodies induced by infection or vaccination, although with moderate efficiency. Collectively, our study reveals that antibody evasion of B.1.617 may contribute to the rapid spread of this variant.

INTRODUCTION

The severe acute respiratory syndrome coronavirus 2 (SARS-CoV-2) is the causative agent of the devastating coronavirus disease 2019 (COVID-19) pandemic, which more than one year after its emergence is associated with record numbers in cases and deaths (W.H.O., 2021). Effective antivirals are largely lacking, although recombinant antibodies targeting the viral spike protein (S) can significantly reduce viral load und have received emergency use authorization (EUA) (Chen et al., 2021a; Gottlieb et al., 2021). Drugs that target the dysregulated cytokine responses characteristic for COVID-19 are available but their clinical benefit is oversee-able (Tomazini et al., 2020; W.H.O. REACT Working Group et al., 2020). While progress in treatment development is moderate, mRNA- and vector-based vaccines are available that provide efficient protection against disease (Baden et al., 2021; Polack et al., 2020). As a consequence, vaccination is viewed as the key instrument in combating and ultimately ending the COVID-19 pandemic.

Strategies to fight the COVID-19 pandemic either by vaccines or non-pharmaceutical interventions have been threatened by the emergence of SARS-CoV-2 variants of concern (VOC). These variants harbor mutations that confer increased transmissibility or immune evasion (Plante et al., 2021). Studies of mutations present in VOC have mainly focused on the viral S protein. The S protein is incorporated into the viral membrane and facilitates viral entry into target cells. For this, the surface unit, S1, of the S protein first binds to the cellular receptor ACE2 (Hoffmann et al., 2020; Zhou et al., 2020) via its receptor binding domain (RBD). Subsequently, the S protein is activated by TMPRSS2 or related cellular proteases (Hoffmann et al., 2021b; Hoffmann et al., 2020) and the transmembrane unit, S2, of the S protein facilitates fusion of the viral and a cellular membrane, allowing delivery of the viral genome into the host cell. These processes are essential for SARS-CoV-2 infection and are targeted by drugs and neutralizing antibodies.

The prototypic VOC with increased fitness is variant B.1.1.7, which emerged in the United Kingdom and is now spreading in many countries. B.1.1.7 replicates to higher levels in patients and is more efficiently transmitted between humans as compared to the previously circulating viruses (Frampton et al., 2021; Graham et al., 2021; Leung et al., 2021). The increased transmissibility might be linked to mutation N501Y in the RBD that might increase binding to ACE2 (Ali et al., 2021; Luan et al., 2021). However, the exact mechanisms underlying more robust transmission of B.1.1.7 remain to be elucidated. In contrast, differences in antibody-mediated neutralization between previously circulating viruses and variant B.1.1.7 are minor, with B.1.1.7 being slightly less sensitive to neutralization (Chen et al., 2021b; Collier et al., 2021; Hoffmann et al., 2021a; Kuzmina et al., 2021; Muik et al., 2021; Planas et al., 2021; Shen et al., 2021; Supasa et al., 2021; Wang et al., 2021a; Xie et al., 2021). In sum, B.1.1.7 shows increased fitness and will outcompete previously circulating viruses in an immunologically naïve population.

In populations with a high percentage of individuals with pre-existing immune responses against SARS-CoV-2, viral variants that can evade immune control have a selective advantage. Variant B.1.351 that became dominant in South Africa (Tegally et al., 2021) and variant P.1 that became dominant in Brazil (Faria et al., 2021) are such variants (Chen et al., 2021b; Dejnirattisai et al., 2021; Edara et al., 2021; Garcia-Beltran et al., 2021; Hoffmann et al., 2021a; Kuzmina et al., 2021; Planas et al., 2021; Wang et al., 2021a; Zhou et al., 2021). These variants harbor mutations in the S protein that reduce neutralization by antibodies, including E484K, which is located in the RBD and is present in both, B.1.351 and P1 (Li et al., 2021; Liu et al., 2021; Wang et al., 2021c). At present, evasion form antibodies is most prominent for variant B.1.351 but it is unclear whether variants can arise that exhibit increased or even complete neutralization resistance.

India has seen a steep increase in COVID-19 cases and deaths in the recent weeks (W.H.O., 2021). It is believed that many cases are due to infection with a novel variant, B.1.617, that harbors eight mutations in the S protein, including mutations L452R and E484Q within the RBD, which introduce changes at amino acid positions known to modulate antibody-mediated neutralization (Li et al., 2021; Li et al., 2020). However, it is at present unknown whether B.1.617 evades antibody-mediated neutralization. Similarly, it is unknown whether the variant exhibits an altered dependence on host cell factors for entry, which may alter cell tropism, entry efficiency and sensitivity to entry inhibitors.

Here, we report that the S protein of B.1.617 mediates moderately enhanced entry into the human lung- and intestine-derived cell lines Calu-3 and Caco-2, respectively, and that entry is inhibited by soluble ACE2 and Camostat, the latter of which targets TMPRSS2. In contrast, entry driven by the B.1.617 S protein was fully resistant to neutralization by a monoclonal antibody with EUA for COVID-19 treatment (Bamlanivimab). Finally, B.1.617 S protein-driven entry was partially resistant against neutralization by antibodies elicited upon infection or vaccination with the Comirnaty/BNT162b2 vaccine.

RESULTS

The S protein of variant B.1.617 mediates increased entry into certain human intestinal and lung cell lines

The S protein of SARS-CoV-2 variant B.1.617 (GISAID Accession ID: PI_ISL_1360382) harbors a total of eight mutations compared to the S proteins of the viruses sampled at the start of the pandemic (Figure 1). Seven mutations are located within the S1 subunit, three of which are present in the N-terminal domain (R21T, E154K, Q218H), two in the RBD (L452R, E484Q) and two between the RBD and the S1/S2 border (D614G, P681R). One additional mutation is located within the S2 subunit (H1101D) (Figure 1). Since the rapid spread of variant B.1.617 in India might be due to an increased ability to enter cells or to infect a broader range of target cells, we analyzed the cell tropism and entry efficiency of variant B.1.617. For this, we employed vesicular stomatitis virus (VSV) particles pseudotyped with the S protein of either wildtype (WT) SARS-CoV-2 (Wuhan-1 isolate with D614G exchange) or variants B.1.617 or B.1.351. These pseudotyped particles faithfully mimic cell entry of SARS-CoV-2 and have been previously used to identify host factors required for SARS-CoV-2 cell entry and to study neutralization of SARS-CoV-2 by antibodies (Hoffmann et al., 2021a; Hoffmann et al., 2020; Riepler et al., 2020; Schmidt et al., 2020).

We analyzed a total of eight cell lines - Vero, Caco-2, Calu-3, Calu-3 (ACE2), 293T, A549 (ACE2), A549 (ACE2+TMPRSS2) and Huh-7 - most of which are commonly used as cell culture models for various aspects of SARS-CoV-2 replication. Calu-3 (ACE2), A549 (ACE2) and A549 (ACE2+TMPRSS2) cells were engineered to express ACE2 or ACE2 in conjunction with TMPRSS2.

For most cell lines we did not observe significant differences in cell entry efficiency between the WT and variant S proteins (Figure 2A and Figure S1). The only exceptions were Caco-2 and Calu-3 cells (and 293T cells in case of B.1.351), which are derived from human intestine and lung, respectively, and for which the S protein of B.1.617 (and B.1.351) mediated entry with moderately increased efficiency (Figure 2A and Figure S1). Of note this increase was less prominent when Calu-3 cells were engineered to overexpress ACE2. In addition, we investigated S protein-driven cell entry into BHK-21 cells, which were transfected either with empty plasmid or ACE2 expression plasmid. As expected, BHK-21 cells transfected with empty plasmid did not allow entry driven by any of the S proteins tested but were efficiently entered by particles bearing the VSV glycoprotein (VSV-G) (Figure 2B). In contrast, directed ACE2 expression rendered these cells susceptible to S protein-driven entry and entry efficiency was comparable between WT, B.1.351 and B.1.617 S proteins (Figure 2B). In sum, we demonstrate that the S protein of SARS-CoV-2 B.1.617 allows for moderately enhanced entry into certain cells of the respiratory and digestive tracts.

Soluble ACE2 and Camostat inhibit cell entry driven by the S protein of variant B.1.617

We next examined whether entry of B.1.617 can be blocked by inhibitors targeting the RBD (soluble ACE2) and proteolytic activation (Camostat) of the S protein. Soluble ACE2 binds to the RBD and blocks subsequent engagement of membrane bound ACE2. It inhibits SARS-CoV and SARS-CoV-2 cell entry and is being developed for COVID-19 treatment (Kuba et al., 2005; Monteil et al., 2020). Soluble ACE2 blocked Caco-2 cell entry driven by WT, B.1.351 and B.1.617 S proteins with comparable efficiency but did not interfere with entry driven by VSV-G (Figure 3A). Similar results were obtained for Camostat, a clinically-proven serine protease

inhibitor active against TMPRSS2 (Hoffmann et al., 2020) (Figure 3B). These results indicate that soluble ACE2 and Camostat will be active against the B.1617 variant.

Resistance against the therapeutic antibody Bamlanivimab.

The neutralizing monoclonal antibodies Casirivimab (REGN10933), Imdevimab (REGN10987) and Bamlanivimab (LY-CoV555) and Etesevimab (LY-CoV016) (Figure S2) have received EUA for COVID-19 therapy. We analyzed whether these antibodies were able to inhibit host cell entry driven by the S protein of variant B.1.617. An irrelevant control antibody (hIgG) failed to block entry mediated by all viral glycoproteins tested (Figure 4), as expected. Casirivimab inhibited host cell entry mediated by the S protein of B.1.351 with reduced efficiency, in keeping with published data (Hoffmann et al., 2021a), and also inhibition of B.1.617 S protein-driven entry was diminished (Figure 4), in keeping with the presence of mutations in the antibody binding site (Figure S2). In contrast, B.1.351 and B.1.617 S protein-mediated entry was efficiently inhibited by Imdevimab and by a cocktail of Casirivimab and Imdevimab, termed REGN-COV (Figure 4). Further, Bamlanivimab failed to inhibit entry driven by the S protein of variant B.1.351, as expected (Hoffmann et al., 2021a), and was also unable to block entry driven by the S protein of variant B.1.617 (Figure 4). Bamlanivimab resistance of B.1.617 is in agreement with mutations in the epitope recognized by the antibody (Figure S2). Etesevimab blocked entry driven by WT and B.1.617 S proteins with comparable efficiency but failed to inhibit B.1.351 S protein-driven cell entry (Figure 4). Finally, a cocktail of Bamlanivimab and Etesevimab was less effective in inhibiting B.1.617 S protein-driven cell entry compared to WT SARS-CoV-2 S and completely failed to block entry driven by B.1.351 S (Figure 4). These results suggest that Casirivimab and particularly Bamlanivimab monotherapy may not be suitable for treatment of patients infected with variant B1.617.

Diminished neutralization by plasma from COVID-19 convalescent patients

SARS-CoV-2 infection induces the generation of neutralizing antibodies in most infected patients and it is believed that these antibody responses are important for protection from re-infection (Rodda et al., 2021; Wajnberg et al., 2020). Therefore, we determined whether variant B.1.617 evades inhibition by antibodies, which might contribute to its increasing transmission dynamics. For this, we analyzed antibody-mediated neutralization using plasma samples obtained from 15 COVID-19 patients at the intensive care unit of Göttingen University Hospital (Table S1). These plasma samples were prescreened for neutralizing activity and tested for their ability to block host cell entry driven by WT S protein and the S protein of variant B.1.617. The S protein of variant B.1.351 served as control since this S protein efficiently evades antibody-mediated neutralization (Hoffmann et al., 2021a). Inhibition of entry driven by the B.1.351 S protein was almost 6-fold less efficient as compared to WT S protein (Figure 5A and Figure S3A). Neutralization of particles bearing the S protein of variant B.1.617 was also reduced but the reduction was less prominent (~ 2-fold) (Figure 5A and Figure S3A). These results suggest that variant B.1.617 might evade antibody-mediated control in COVID-19 convalescent patients, although with moderate efficiency.

Diminished neutralization by plasma from Comirnaty/BNT162b2 vaccinated patients

Vaccination with Comirnaty/BNT162b2 has been shown to be safe and to protect against COVID-19 with high efficiency (Polack et al., 2020). The vaccine is based on an mRNA that encodes the SARS-CoV-2 S protein. The vaccine induces antibody and T cell responses (Grifoni et al., 2020; Peng et al., 2020) and the neutralizing antibodies triggered by vaccination are believed to be important for vaccine-induced protection against SARS-CoV-2 infection.

Therefore, we analyzed whether cell entry driven by the S protein of variant B.1.617 can be efficiently inhibited by plasma from Comirnaty/BNT162b2 vaccinated individuals (Table S2). To address this question, we analyzed neutralization by 15 plasma samples obtained from vaccinees two to three weeks after they had received the second vaccine dose. All sera efficiently inhibited entry driven by WT S protein (Figure 5B and Figure S3B). Inhibition of entry driven by B.1.351 S protein was more than 11-fold reduced as compared to WT (Figure 5B), in keeping with expectations (Hoffmann et al., 2021a). Entry mediated by the S protein of variant B.1.617 was also less efficiently inhibited but evasion from antibody-mediated inhibition was less pronounced (~ 3-fold reduction) (Figure 5B). Thus, variant B.1.617 can partially evade control by antibodies induced by vaccination with Comirnaty/BNT162b2.

DISCUSSION

The recent surge in COVID-19 cases and deaths in India is paralleled by the spread of the novel SARS-CoV-2 variant B.1.617. This variant harbors mutations in the RBD and other parts of the S protein that might alter important biological properties of the virus, including the efficiency of entry into target cells and the susceptibility to drugs and antibodies targeting the entry process. The present study reveals that the B.1.617 S protein can facilitate entry into Calu-3 lung and Caco-2 colon cells with slightly increased efficiency and shows that entry can be blocked by soluble ACE2 and Camostat. In contrast, Bamlanivimab, a recombinant antibody with EUA did not inhibit entry driven by the B.1.617 S protein and evidence for moderate evasion of antibodies induced by infection and Comirnaty/BNT162b2 vaccination was obtained.

The spread of variant B.1.617 in India might be partially due to increased fitness of this variant, i.e. an increased ability to amplify in patients and to be transmitted between patients. Augmented fitness has been documented for SARS-CoV-2 variant B.1.1.7 (Frampton et al., 2021; Graham et al., 2021; Leung et al., 2021) but the underlying mechanism is unclear. Increased host cell entry due to more efficient ACE2 binding or more robust proteolytic activation of the S protein might contribute to augmented fitness. Host cell entry driven by the B.1.617 S protein was not increased when cell lines were examined that expressed moderate levels of endogenous ACE2, like 293T cells, arguing against more efficient ACE2 usage by variant B.1.617. Similarly, the comparable inhibition of particles bearing WT or B.1.617 S protein by soluble ACE2 points towards no substantial differences in ACE2 binding efficiency. However, the B.1.617 S protein facilitated moderately increased entry into the human lung and intestinal cell lines Calu-3 and Caco-2, respectively, and this effect was much less pronounced when ACE2 was overexpressed in Calu-3 cells. Therefore, one can speculate that B.1.617 may have an increased ability to use certain entry augmenting factors that are expressed in a cell type

specific fashion. Potential candidates are heparan sulfate (Clausen et al., 2020), Axl (Wang et al., 2021b) and neuropilin-1 (Cantuti-Castelvetri et al., 2020).

Another explanation for the increased spread of variant B.1.617 in India might be immune evasion, i.e. the ability to spread in a population in which a substantial portion of individuals has preexisting immune responses against SARS-CoV-2. This is the case in India, at least in certain areas or resource-poor communities, in which seroprevalence can be higher than 70% (Kar et al., 2021; Malani et al., 2021; Mohanan et al., 2021). The RBD of the B.1.617 S protein harbors two mutations associated with (L452R) or suspected (E484Q) of antibody evasion. Thus, mutation L452R was previously shown to facilitate escape from neutralizing antibodies (Li et al., 2020). Moreover, E484K present the B.1.351 and P.1 variants confers antibody resistance (Li et al., 2021) and one could speculate that exchange E484Q might have a similar effect. In fact, both L452R and E484K are likely responsible for B.1.617 resistance to Bamlanivimab (Starr et al., 2021) (Figure S2). In the light of these findings it was not unexpected that evasion of the B.1.617 S protein from antibodies in plasma from COVID-19 convalescent patients and Comirnaty/BNT162b2 vaccinated individuals was observed. However, evasion from antibody-mediated neutralization by B.1.617 S was clearly less pronounced as compared to the S protein of the B.1.351 variant. Differences between these variants regarding the additional mutations located in and outside of the RBD likely account for their differential neutralization sensitivity.

Collectively, our results suggest that although B.1.617 may be able to evade control by antibodies to some extend other factors might contribute to its fast spread, including a potential fitness benefit or reduced adherence to COVID-19 protection measures (e.g. mask wearing and social distancing).

ACKNOWLEDGMENTS

We like to thank Roberto Cattaneo, Georg Herrler, Stephan Ludwig, Andrea Maisner, Thomas Pietschmann and Gert Zimmer for providing reagents. We gratefully acknowledge the originating laboratories responsible for obtaining the specimens and the submitting laboratories where genetic sequence data were generated and shared via the GISAID Initiative, on which this research is based. J.M. acknowledges funding by a Collaborative Research Centre grant of the German Research Foundation (316249678 – SFB 1279), the European Union's Horizon 2020 research and innovation programme under grant agreement No 101003555 (Fight-nCoV) and the Federal Ministry of Economics, Germany (Combi-CoV-2). S.P. acknowledges funding by BMBF (RAPID Consortium, 01KI1723D and 01KI2006D; RENACO, 01KI20328A, 01KI20396, COVIM consortium), the county of Lower Saxony and the German Research Foundation (DFG). N.K. acknowledges funding by BMBF (ANI-CoV, 01KI2074A). M.S.W. received unrestricted funding from Sartorius AG, Lung research.

AUTHOR CONTRIBUTIONS

Conceptualization, M.H., S.P.; Funding acquisition, S.P.; Investigation, M.H., H.H.-W., N.K., A.K., I.N., L.G., A.S., A.-S.M.; Essential resources, M.S.W., S.S., H.-M.J., M.V.S., G.M.N.B.; Writing, M.H., S.P.; Review and editing, all authors.

DECLARATION OF INTEREST

The authors declare not competing interests

MATERIALS AND METHODS

Cell culture

293T (human, female, kidney; ACC-635, DSMZ, RRID: CVCL_0063), Huh-7 (human, male, liver; JCRB0403, JCRB; RRID: CVCL_0336, kindly provided by Thomas Pietschmann, TWINCORE, Centre for Experimental and Clinical Infection Research, Hannover, Germany), BHK-21 (Syrian hamster, male, kidney; ATCC Cat# CCL-10; RRID: CVCL_1915, kindly provided by Georg Herrler, University of Veterinary Medicine, Hannover, Germany) and Vero76 cells (African green monkey, female, kidney; CRL-1586, ATCC; RRID: CVCL_0574, kindly provided by Andrea Maisner, Institute of Virology, Philipps University Marburg, Marburg, Germany) were cultivated in Dulbecco's modified Eagle medium (DMEM) supplemented with 10% fetal bovine serum (FCS, Biochrom or GIBCO), 100 U/ml of penicillin and 0.1 mg/ml of streptomycin (PAN-Biotech). Caco-2 (human, male, intestine; HTB-37, ATCC, RRID:CVCL_0025), Calu-3 (human, male, lung; HTB-55, ATCC; RRID: CVCL_0609, kindly provided by Stephan Ludwig, Institute of Virology, University of Münster, Germany) and Calu-3 cells stably overexpressing ACE2, Calu-3 (ACE2) (Hoffmann et al., 2021c), were cultivated in minimum essential medium supplemented with 10% FCS, 100 U/ml of penicillin and 0.1 mg/ml of streptomycin (PAN-Biotech), 1x non-essential amino acid solution (from 100x stock, PAA) and 1 mM sodium pyruvate (Thermo Fisher Scientific). Calu-3 (ACE2) cells further received 0.5 µg/ml puromycin (Invivogen). A549-ACE2 (Hoffmann et al., 2021a) and A549-ACE2/TMPRSS2 cells (Hoffmann et al., 2021a) were derived from parental A549 cells (human, male, lung; CRM-CCL-185, ATCC, RRID:CVCL_0023; kindly provided by Georg Herrler) and cultivated in DMEM/F-12 Medium (ThermoFisher Scientific) supplemented with 10% FCS, 100 U/ml of penicillin and 0.1 mg/ml of streptomycin (PAN-Biotech), 1x non-essential amino acid

335 solution (from 100x stock, PAA), 1 mM sodium pyruvate (Thermo Fisher Scientific) and 0.5
336 µg/ml puromycin (Invivogen). A549-ACE2/TMPRSS2 cells further received 1 µg/ml blasticidin
337 (Invivogen).

338 All cell lines were incubated at 37 °C in a humidified atmosphere containing 5% CO_2.
339 Authentication of cell lines was performed by STR-typing, amplification and sequencing of a
340 fragment of the cytochrome c oxidase gene, microscopic examination and/or according to their
341 growth characteristics. In addition, cell lines were routinely tested for contamination by
342 mycoplasma.

343

344 **Expression plasmids**

345 Expression plasmids for DsRed (Hoffmann et al., 2020), vesicular stomatitis virus (VSV,
346 serotype Indiana) glycoprotein (VSV-G) (Brinkmann et al., 2017), WT SARS-CoV-2 S (codon-
347 optimized, based on the Wuhan/Hu-1/2019 isolate, contains D614G exchange; with a C-terminal
348 truncation of 18 amino acid) (Hoffmann et al., 2021a), SARS-CoV-2 S B.1.351 (codon-
349 optimized; with a C-terminal truncation of 18 amino acid) (Hoffmann et al., 2021a), angiotensin-
350 converting enzyme 2 (ACE2) (Hoffmann et al., 2013) and soluble ACE2 (Hoffmann et al.,
351 2021a) have been described before. In order to generate the expression vector for the S protein of
352 SARS-CoV-2 variant B.1.617, the required mutations were inserted into the WT SARS-CoV-2 S
353 sequence by overlap extension PCR. The resulting open reading frame was further inserted into
354 the pCG1 plasmid (kindly provided by Roberto Cattaneo, Mayo Clinic College of Medicine,
355 Rochester, MN, USA), making use of the unique BamHI and XbaI restriction sites. Sequence
356 integrity was verified by sequencing using a commercial sequencing service (Microsynth
357 SeqLab). Specific cloning details (e.g., primer sequences and restriction sites) are available upon
358 request. Transfection of 293T cells was carried out by the calcium-phosphate precipitation

359 method, while BHK-21 cells were transfected using Lipofectamine LTX (Thermo Fisher
360 Scientific).
361
362 **Sequence analysis and protein models**
363 The S protein sequence of SARS-CoV-2 S variant B.1.617 (GISAID Accession ID:
364 PI_ISL_1360382) was obtained from the GISAID (global initiative on sharing all influenza data)
365 database (https://www.gisaid.org/). Protein models were generated using the YASARA software
366 (http://www.yasara.org/index.html) and are based on PDB: 6XDG (Hansen et al., 2020),PDB:
367 7L3N (Jones et al., 2020) or PDB: 7C01 (Shi et al., 2020), or a template that was constructed by
368 modelling the SARS-2-S sequence on PDB: 6XR8 (Cai et al., 2020), using the SWISS-MODEL
369 online tool (https://swissmodel.expasy.org/).
370
371 **Preparation of vesicular stomatitis virus pseudotypes**
372 For this study, we employed rhabdoviral pseudotype particles that are based on a replication-
373 deficient VSV vector that lacks the genetic information for VSV-G and instead codes for two
374 reporter proteins, enhanced green fluorescent protein and firefly luciferase (FLuc), VSV∗ΔG-
375 FLuc (kindly provided by Gert Zimmer, Institute of Virology and Immunology, Mittelhäusern,
376 Switzerland) (Berger Rentsch and Zimmer, 2011). Pseudotyping of VSV∗ΔG-FLuc was carried
377 out according to a published protocol (Kleine-Weber et al., 2019). First, 293T cells that expressed
378 the respective S protein, VSV-G (or no viral protein, control) following transfection were
379 inoculated with VSV∗ΔG-FLuc at a multiplicity of infection of three and incubated for 1 h at 37
380 °C. Next, the inoculum was aspirated and cells were washed with phosphate-buffered saline
381 (PBS). Thereafter, cells received culture medium containing anti-VSV-G antibody (culture
382 supernatant from I1-hybridoma cells; ATCC no. CRL-2700; except for cells expressing VSV-G,

which received only medium) and incubated for 16-18 h. Then, pseudotype particles were harvested. For this, the culture supernatant was collected and centrifuged (2,000 x g, 10 min, room temperature) in order to pellet cellular debris. Finally, the clarified supernatant was aliquoted and stored at -80 °C.

Production of soluble ACE2

For the production of soluble ACE2 fused to the Fc portion of human immunoglobulin G (IgG), sol-ACE2, 293T cells were grown in a T-75 flask and transfected with 20 µg of sol-ACE2 expression plasmid. The medium was exchanged at 10 h posttransfection and cells were further incubated for 38 h. Then, the culture supernatant was collected and the cells received fresh medium and were further incubated. The collected supernatant was further centrifuged (2,000 x g, 10 min, 4 °C) and stored at 4 °C. After an additional 24 h, the culture supernatant was harvested and centrifuged as described before. Next, the clarified supernatants from both harvests were combined, loaded onto Vivaspin protein concentrator columns with a molecular weight cut-off of 30 kDa (Sartorius) and centrifuged at 4,000 x g at 4 °C until a concentration factor of 20 was achieved. Finally, the concentrated sol-ACE2 was aliquoted and stored at -80 °C.

Collection of serum and plasma samples

All plasma samples were heat-inactivated (56 °C, 30 min) before analysis. Further, all plasma were pre-screened for the presence of neutralizing activity against WT SARS-CoV-2 S using a pseudotype neutralization test. Convalescent plasma samples were collected from COVID-19 patients treated at the intensive care unit of the University Medicine Göttingen under approval given by the ethic committee of the University Medicine Göttingen (SeptImmun Study 25/4/19 Ü). For collection of convalescent plasma, Cell Preparation Tube (CPT) vacutainers with sodium

citrate were used and plasma was collected as supernatant over the PBMC layer. Plasma from individuals vaccinated with BioNTech/Pfizer vaccine BNT162b2/ Comirnaty were obtained 24-31 days after the second dose. The study was approved by the Institutional Review Board of Hannover Medical School (8973_BO_K_2020). For vaccinated patients, blood was collected in S-Monovette® EDTA tubes (Sarstedt).

Transduction of target cells

All transduction experiments were carried out in 96-well format at a cell confluency of 50-80%. For experiments addressing cell tropism and entry efficiency, Vero, Caco-2, Calu-3, Calu-3 (ACE2), 293T, A549 (ACE2), A549 (ACE2+TMPRSS2) and Huh-7 target cells were inoculated with identical volumes of pseudotype preparations. BHK-21 cells were transfected 24 h prior to pseudotype inoculation with either empty plasmid or ACE2 expression plasmid (0.1 µg/well) using Lipofectamine LTX (Thermo Fisher Scientific). In order to study the antiviral activity of Camostat mesylate, Caco-2 target cells, which express endogenous TMPRSS2, were pre-incubated for 1 h with medium containing different concentrations (100, 10, 1, 0.1 or 0.01 µM) of Camostat mesylate (prepared from a 100 mM stock; Tocris) or the solvent dimethyl sulfoxide (DMSO, 1:1,000; Sigma-Aldrich) as control before being inoculated with VSV bearing S protein, VSV-G or no glycoprotein. For experiments addressing the antiviral activity of soluble ACE2, pseudotype particles bearing S protein, VSV-G or no protein were pre-incubated with different amounts of concentrated sol-ACE2 (final sol-ACE2 dilutions in the mixtures: undiluted, 1:10, 1:100, 1:1,000:10,000) or only medium for 30 min at 37 °C, before the mixtures were added onto Caco-2 cells. In all cases, transduction efficiency was determined at 16-18 h postinoculation. For this, the culture supernatant was aspirated. Next, cells were lysed in PBS containing 0.5% Triton-X-100 (Carl Roth) for 30 min at room temperature. Thereafter, cell lysates were transferred into

white 96-well plates. Finally, FLuc activity was measured using a commercial substrate (Beetle-Juice, PJK; Luciferase Assay System, Promega) and Hidex Sense Plate Reader (Hidex).

Pseudotype particle neutralization test

For neutralization experiments, S protein bearing pseudotype particles were pre-incubated for 30 min at 37 °C with different concentrations of monoclonal antibodies (Casirivimab, Imdevimab, Casirivimab+Imdevimab [1:1], Bamlanivimab, Esetevimab, Bamlanivimab+Etesevimab [1:1] or unrelated control IgG [2, 0.2, 0.02, 0.002, 0.0002, 0.00002 µg/ml]) or plasma samples obtained from convalescent COVID-19 patients or individuals vaccinated with the Pfizer/BioNTech vaccine BNT162b2/Comirnaty (1:25, 1:100, 1:400, 1:1,600, 1:6,400, 1:25,600), before the mixtures were inoculated onto Vero cells. In all cases, particles incubated only with medium served as control. Transduction efficiency was determined at 16-18 h postinoculation as described above.

Data analysis

The results presented in this study represent average (mean) data obtained from three biological replicates, each conducted with technical quadruplicates. The only exception are the neutralization data involving plasma from infected/vaccinated individuals, which are based on a single experiment (standard in the field), conducted with technical quadruplicates. Error bars are defined as either standard deviation (SD, neutralization data involving plasma from infected/vaccinated individuals) or standard error of the mean (SEM, all other data). Data ware analyzed using Microsoft Excel (as part of the Microsoft Office software package, version 2019, Microsoft Corporation) and GraphPad Prism 8 version 8.4.3 (GraphPad Software).

Data normalization was performed in the following fashion: (i) For comparison of entry efficiency by the different S proteins, transduction was normalized against WT SARS-CoV-2 S (set as 100%). Alternatively, transduction was normalized against the background signal (luminescence measured for cells inoculated with particles bearing no viral glycoprotein; set as 1). (ii) In order to investigate inhibition of S protein-driven cell entry by sol-ACE2, Camostat mesylate, monoclonal antibodies or plasma from infected/vaccinated individuals, transduction was normalized against a reference sample (e.g., control-treated cells or pseudotypes, set as 0% inhibition).

The neutralizing titer 50 (NT50) value, which indicates the plasma dilution that causes a 50 % reduction of transduction efficiency, was calculated using a non-linear regression model (inhibitor vs. normalized response, variable slope). Statistical significance was tested by one- or two-way analysis of variance (ANOVA) with Dunnett's post-hoc test, paired Students t-test or by multiple t-test with correction for multiple comparison (Holm-Sidak method). Only p values of 0.05 or lower were considered statistically significant ($p > 0.05$, not significant [ns]; $p \leq 0.05$, *; $p \leq 0.01$, **; $p \leq 0.001$, ***). The details on the statistical test and the error bars are specified in the figure legends.

478 **REFERENCES**
479
480 Ali, F., Kasry, A., and Amin, M. (2021). The new SARS-CoV-2 strain shows a stronger binding
481 affinity to ACE2 due to N501Y mutant. Med Drug Discov *10*, 100086.

482 Baden, L.R., El Sahly, H.M., Essink, B., Kotloff, K., Frey, S., Novak, R., Diemert, D., Spector,
483 S.A., Rouphael, N., Creech, C.B.*, et al.* (2021). Efficacy and Safety of the mRNA-1273 SARS-
484 CoV-2 Vaccine. N Engl J Med *384*, 403-416.

485 Berger Rentsch, M., and Zimmer, G. (2011). A vesicular stomatitis virus replicon-based bioassay
486 for the rapid and sensitive determination of multi-species type I interferon. PLoS One *6*, e25858.

487 Brinkmann, C., Hoffmann, M., Lubke, A., Nehlmeier, I., Kramer-Kuhl, A., Winkler, M., and
488 Pohlmann, S. (2017). The glycoprotein of vesicular stomatitis virus promotes release of virus-like
489 particles from tetherin-positive cells. PLoS One *12*, e0189073.

490 Cai, Y., Zhang, J., Xiao, T., Peng, H., Sterling, S.M., Walsh, R.M., Jr., Rawson, S., Rits-Volloch,
491 S., and Chen, B. (2020). Distinct conformational states of SARS-CoV-2 spike protein. Science
492 *369*, 1586-1592.

493 Cantuti-Castelvetri, L., Ojha, R., Pedro, L.D., Djannatian, M., Franz, J., Kuivanen, S., van der
494 Meer, F., Kallio, K., Kaya, T., Anastasina, M.*, et al.* (2020). Neuropilin-1 facilitates SARS-CoV-
495 2 cell entry and infectivity. Science *370*, 856-860.

496 Chen, P., Nirula, A., Heller, B., Gottlieb, R.L., Boscia, J., Morris, J., Huhn, G., Cardona, J.,
497 Mocherla, B., Stosor, V.*, et al.* (2021a). SARS-CoV-2 Neutralizing Antibody LY-CoV555 in
498 Outpatients with Covid-19. N Engl J Med *384*, 229-237.

499 Chen, R.E., Zhang, X., Case, J.B., Winkler, E.S., Liu, Y., VanBlargan, L.A., Liu, J., Errico, J.M.,
500 Xie, X., Suryadevara, N.*, et al.* (2021b). Resistance of SARS-CoV-2 variants to neutralization by
501 monoclonal and serum-derived polyclonal antibodies. Nat Med.

502 Clausen, T.M., Sandoval, D.R., Spliid, C.B., Pihl, J., Perrett, H.R., Painter, C.D., Narayanan, A.,
503 Majowicz, S.A., Kwong, E.M., McVicar, R.N.*, et al.* (2020). SARS-CoV-2 Infection Depends on
504 Cellular Heparan Sulfate and ACE2. Cell *183*, 1043-1057 e1015.

505 Collier, D.A., De Marco, A., Ferreira, I., Meng, B., Datir, R.P., Walls, A.C., Kemp, S.A., Bassi,
506 J., Pinto, D., Silacci-Fregni, C., *et al.* (2021). Sensitivity of SARS-CoV-2 B.1.1.7 to mRNA
507 vaccine-elicited antibodies. Nature.

508 Dejnirattisai, W., Zhou, D., Supasa, P., Liu, C., Mentzer, A.J., Ginn, H.M., Zhao, Y.,
509 Duyvesteyn, H.M.E., Tuekprakhon, A., Nutalai, R., *et al.* (2021). Antibody evasion by the P.1
510 strain of SARS-CoV-2. Cell.

511 Edara, V.V., Norwood, C., Floyd, K., Lai, L., Davis-Gardner, M.E., Hudson, W.H., Mantus, G.,
512 Nyhoff, L.E., Adelman, M.W., Fineman, R., *et al.* (2021). Infection- and vaccine-induced
513 antibody binding and neutralization of the B.1.351 SARS-CoV-2 variant. Cell Host Microbe *29*,
514 516-521 e513.

515 Faria, N.R., Mellan, T.A., Whittaker, C., Claro, I.M., Candido, D.D.S., Mishra, S., Crispim,
516 M.A.E., Sales, F.C.S., Hawryluk, I., McCrone, J.T., *et al.* (2021). Genomics and epidemiology of
517 the P.1 SARS-CoV-2 lineage in Manaus, Brazil. Science.

518 Frampton, D., Rampling, T., Cross, A., Bailey, H., Heaney, J., Byott, M., Scott, R., Sconza, R.,
519 Price, J., Margaritis, M., *et al.* (2021). Genomic characteristics and clinical effect of the emergent
520 SARS-CoV-2 B.1.1.7 lineage in London, UK: a whole-genome sequencing and hospital-based
521 cohort study. Lancet Infect Dis.

522 Garcia-Beltran, W.F., Lam, E.C., St Denis, K., Nitido, A.D., Garcia, Z.H., Hauser, B.M.,
523 Feldman, J., Pavlovic, M.N., Gregory, D.J., Poznansky, M.C., *et al.* (2021). Multiple SARS-
524 CoV-2 variants escape neutralization by vaccine-induced humoral immunity. Cell *184*, 2372-
525 2383 e2379.

526 Gottlieb, R.L., Nirula, A., Chen, P., Boscia, J., Heller, B., Morris, J., Huhn, G., Cardona, J.,
527 Mocherla, B., Stosor, V., *et al.* (2021). Effect of Bamlanivimab as Monotherapy or in
528 Combination With Etesevimab on Viral Load in Patients With Mild to Moderate COVID-19: A
529 Randomized Clinical Trial. JAMA *325*, 632-644.

530 Graham, M.S., Sudre, C.H., May, A., Antonelli, M., Murray, B., Varsavsky, T., Klaser, K.,
531 Canas, L.S., Molteni, E., Modat, M., *et al.* (2021). Changes in symptomatology, reinfection, and

532 transmissibility associated with the SARS-CoV-2 variant B.1.1.7: an ecological study. Lancet
533 Public Health.

534 Grifoni, A., Weiskopf, D., Ramirez, S.I., Mateus, J., Dan, J.M., Moderbacher, C.R., Rawlings,
535 S.A., Sutherland, A., Premkumar, L., Jadi, R.S., *et al.* (2020). Targets of T Cell Responses to
536 SARS-CoV-2 Coronavirus in Humans with COVID-19 Disease and Unexposed Individuals. Cell
537 *181*, 1489-1501 e1415.

538 Hansen, J., Baum, A., Pascal, K.E., Russo, V., Giordano, S., Wloga, E., Fulton, B.O., Yan, Y.,
539 Koon, K., Patel, K., *et al.* (2020). Studies in humanized mice and convalescent humans yield a
540 SARS-CoV-2 antibody cocktail. Science *369*, 1010-1014.

541 Hoffmann, M., Arora, P., Gross, R., Seidel, A., Hornich, B.F., Hahn, A.S., Kruger, N., Graichen,
542 L., Hofmann-Winkler, H., Kempf, A., *et al.* (2021a). SARS-CoV-2 variants B.1.351 and P.1
543 escape from neutralizing antibodies. Cell.

544 Hoffmann, M., Hofmann-Winkler, H., Smith, J.C., Kruger, N., Arora, P., Sorensen, L.K.,
545 Sogaard, O.S., Hasselstrom, J.B., Winkler, M., Hempel, T., *et al.* (2021b). Camostat mesylate
546 inhibits SARS-CoV-2 activation by TMPRSS2-related proteases and its metabolite GBPA exerts
547 antiviral activity. EBioMedicine *65*, 103255.

548 Hoffmann, M., Kleine-Weber, H., Schroeder, S., Kruger, N., Herrler, T., Erichsen, S.,
549 Schiergens, T.S., Herrler, G., Wu, N.H., Nitsche, A., *et al.* (2020). SARS-CoV-2 Cell Entry
550 Depends on ACE2 and TMPRSS2 and Is Blocked by a Clinically Proven Protease Inhibitor. Cell
551 *181*, 271-280 e278.

552 Hoffmann, M., Muller, M.A., Drexler, J.F., Glende, J., Erdt, M., Gutzkow, T., Losemann, C.,
553 Binger, T., Deng, H., Schwegmann-Wessels, C., *et al.* (2013). Differential sensitivity of bat cells
554 to infection by enveloped RNA viruses: coronaviruses, paramyxoviruses, filoviruses, and
555 influenza viruses. PLoS One *8*, e72942.

556 Hoffmann, M., Zhang, L., Kruger, N., Graichen, L., Kleine-Weber, H., Hofmann-Winkler, H.,
557 Kempf, A., Nessler, S., Riggert, J., Winkler, M.S., *et al.* (2021c). SARS-CoV-2 mutations
558 acquired in mink reduce antibody-mediated neutralization. Cell Rep *35*, 109017.

559 Jones, B.E., Brown-Augsburger, P.L., Corbett, K.S., Westendorf, K., Davies, J., Cujec, T.P.,
560 Wiethoff, C.M., Blackbourne, J.L., Heinz, B.A., Foster, D.*, et al.* (2020). LY-CoV555, a rapidly
561 isolated potent neutralizing antibody, provides protection in a non-human primate model of
562 SARS-CoV-2 infection. bioRxiv.

563 Kar, S.S., Sarkar, S., Murali, S., Dhodapkar, R., Joseph, N.M., and Aggarwal, R. (2021).
564 Prevalence and Time Trend of SARS-CoV-2 Infection in Puducherry, India, August-October
565 2020. Emerg Infect Dis *27*, 666-669.

566 Kleine-Weber, H., Elzayat, M.T., Wang, L., Graham, B.S., Muller, M.A., Drosten, C., Pohlmann,
567 S., and Hoffmann, M. (2019). Mutations in the Spike Protein of Middle East Respiratory
568 Syndrome Coronavirus Transmitted in Korea Increase Resistance to Antibody-Mediated
569 Neutralization. J Virol *93*.

570 Kuba, K., Imai, Y., Rao, S., Gao, H., Guo, F., Guan, B., Huan, Y., Yang, P., Zhang, Y., Deng,
571 W.*, et al.* (2005). A crucial role of angiotensin converting enzyme 2 (ACE2) in SARS
572 coronavirus-induced lung injury. Nat Med *11*, 875-879.

573 Kuzmina, A., Khalaila, Y., Voloshin, O., Keren-Naus, A., Boehm-Cohen, L., Raviv, Y., Shemer-
574 Avni, Y., Rosenberg, E., and Taube, R. (2021). SARS-CoV-2 spike variants exhibit differential
575 infectivity and neutralization resistance to convalescent or post-vaccination sera. Cell Host
576 Microbe *29*, 522-528 e522.

577 Leung, K., Shum, M.H., Leung, G.M., Lam, T.T., and Wu, J.T. (2021). Early transmissibility
578 assessment of the N501Y mutant strains of SARS-CoV-2 in the United Kingdom, October to
579 November 2020. Euro Surveill *26*.

580 Li, Q., Nie, J., Wu, J., Zhang, L., Ding, R., Wang, H., Zhang, Y., Li, T., Liu, S., Zhang, M.*, et al.*
581 (2021). SARS-CoV-2 501Y.V2 variants lack higher infectivity but do have immune escape. Cell
582 *184*, 2362-2371 e2369.

583 Li, Q., Wu, J., Nie, J., Zhang, L., Hao, H., Liu, S., Zhao, C., Zhang, Q., Liu, H., Nie, L.*, et al.*
584 (2020). The Impact of Mutations in SARS-CoV-2 Spike on Viral Infectivity and Antigenicity.
585 Cell *182*, 1284-1294 e1289.

586 Liu, Z., VanBlargan, L.A., Bloyet, L.M., Rothlauf, P.W., Chen, R.E., Stumpf, S., Zhao, H.,
587 Errico, J.M., Theel, E.S., Liebeskind, M.J., *et al.* (2021). Identification of SARS-CoV-2 spike
588 mutations that attenuate monoclonal and serum antibody neutralization. Cell Host Microbe *29*,
589 477-488 e474.

590 Luan, B., Wang, H., and Huynh, T. (2021). Enhanced binding of the N501Y-mutated SARS-
591 CoV-2 spike protein to the human ACE2 receptor: insights from molecular dynamics simulations.
592 FEBS Lett.

593 Malani, A., Shah, D., Kang, G., Lobo, G.N., Shastri, J., Mohanan, M., Jain, R., Agrawal, S.,
594 Juneja, S., Imad, S., *et al.* (2021). Seroprevalence of SARS-CoV-2 in slums versus non-slums in
595 Mumbai, India. Lancet Glob Health *9*, e110-e111.

596 Mohanan, M., Malani, A., Krishnan, K., and Acharya, A. (2021). Prevalence of SARS-CoV-2 in
597 Karnataka, India. JAMA *325*, 1001-1003.

598 Monteil, V., Kwon, H., Prado, P., Hagelkruys, A., Wimmer, R.A., Stahl, M., Leopoldi, A.,
599 Garreta, E., Hurtado Del Pozo, C., Prosper, F., *et al.* (2020). Inhibition of SARS-CoV-2
600 Infections in Engineered Human Tissues Using Clinical-Grade Soluble Human ACE2. Cell *181*,
601 905-913 e907.

602 Muik, A., Wallisch, A.K., Sanger, B., Swanson, K.A., Muhl, J., Chen, W., Cai, H., Maurus, D.,
603 Sarkar, R., Tureci, O., *et al.* (2021). Neutralization of SARS-CoV-2 lineage B.1.1.7 pseudovirus
604 by BNT162b2 vaccine-elicited human sera. Science *371*, 1152-1153.

605 Peng, Y., Mentzer, A.J., Liu, G., Yao, X., Yin, Z., Dong, D., Dejnirattisai, W., Rostron, T.,
606 Supasa, P., Liu, C., *et al.* (2020). Broad and strong memory CD4(+) and CD8(+) T cells induced
607 by SARS-CoV-2 in UK convalescent individuals following COVID-19. Nat Immunol *21*, 1336-
608 1345.

609 Planas, D., Bruel, T., Grzelak, L., Guivel-Benhassine, F., Staropoli, I., Porrot, F., Planchais, C.,
610 Buchrieser, J., Rajah, M.M., Bishop, E., *et al.* (2021). Sensitivity of infectious SARS-CoV-2
611 B.1.1.7 and B.1.351 variants to neutralizing antibodies. Nat Med.

612 Plante, J.A., Mitchell, B.M., Plante, K.S., Debbink, K., Weaver, S.C., and Menachery, V.D.
613 (2021). The variant gambit: COVID-19's next move. Cell Host Microbe *29*, 508-515.

614 Polack, F.P., Thomas, S.J., Kitchin, N., Absalon, J., Gurtman, A., Lockhart, S., Perez, J.L., Perez
615 Marc, G., Moreira, E.D., Zerbini, C.*, et al.* (2020). Safety and Efficacy of the BNT162b2 mRNA
616 Covid-19 Vaccine. N Engl J Med *383*, 2603-2615.

617 Riepler, L., Rossler, A., Falch, A., Volland, A., Borena, W., von Laer, D., and Kimpel, J. (2020).
618 Comparison of Four SARS-CoV-2 Neutralization Assays. Vaccines (Basel) *9*.

619 Rodda, L.B., Netland, J., Shehata, L., Pruner, K.B., Morawski, P.A., Thouvenel, C.D., Takehara,
620 K.K., Eggenberger, J., Hemann, E.A., Waterman, H.R.*, et al.* (2021). Functional SARS-CoV-2-
621 Specific Immune Memory Persists after Mild COVID-19. Cell *184*, 169-183 e117.

622 Schmidt, F., Weisblum, Y., Muecksch, F., Hoffmann, H.H., Michailidis, E., Lorenzi, J.C.C.,
623 Mendoza, P., Rutkowska, M., Bednarski, E., Gaebler, C.*, et al.* (2020). Measuring SARS-CoV-2
624 neutralizing antibody activity using pseudotyped and chimeric viruses. J Exp Med *217*.

625 Shen, X., Tang, H., McDanal, C., Wagh, K., Fischer, W., Theiler, J., Yoon, H., Li, D., Haynes,
626 B.F., Sanders, K.O.*, et al.* (2021). SARS-CoV-2 variant B.1.1.7 is susceptible to neutralizing
627 antibodies elicited by ancestral spike vaccines. Cell Host Microbe.

628 Shi, R., Shan, C., Duan, X., Chen, Z., Liu, P., Song, J., Song, T., Bi, X., Han, C., Wu, L.*, et al.*
629 (2020). A human neutralizing antibody targets the receptor-binding site of SARS-CoV-2. Nature
630 *584*, 120-124.

631 Starr, T.N., Greaney, A.J., Dingens, A.S., and Bloom, J.D. (2021). Complete map of SARS-CoV-
632 2 RBD mutations that escape the monoclonal antibody LY-CoV555 and its cocktail with LY-
633 CoV016. Cell Rep Med *2*, 100255.

634 Supasa, P., Zhou, D., Dejnirattisai, W., Liu, C., Mentzer, A.J., Ginn, H.M., Zhao, Y.,
635 Duyvesteyn, H.M.E., Nutalai, R., Tuekprakhon, A.*, et al.* (2021). Reduced neutralization of
636 SARS-CoV-2 B.1.1.7 variant by convalescent and vaccine sera. Cell *184*, 2201-2211 e2207.

637 Tegally, H., Wilkinson, E., Giovanetti, M., Iranzadeh, A., Fonseca, V., Giandhari, J., Doolabh,
638 D., Pillay, S., San, E.J., Msomi, N., *et al.* (2021). Detection of a SARS-CoV-2 variant of concern
639 in South Africa. Nature *592*, 438-443.

640 Tomazini, B.M., Maia, I.S., Cavalcanti, A.B., Berwanger, O., Rosa, R.G., Veiga, V.C., Avezum,
641 A., Lopes, R.D., Bueno, F.R., Silva, M., *et al.* (2020). Effect of Dexamethasone on Days Alive
642 and Ventilator-Free in Patients With Moderate or Severe Acute Respiratory Distress Syndrome
643 and COVID-19: The CoDEX Randomized Clinical Trial. JAMA *324*, 1307-1316.

644 W.H.O. (2021). Weekly epidemiological update on COVID-19 - 27 April 2021.

645 W.H.O. REACT Working Group, W.H.O.R.E.A.f.C.-T.W.G., Sterne, J.A.C., Murthy, S., Diaz,
646 J.V., Slutsky, A.S., Villar, J., Angus, D.C., Annane, D., Azevedo, L.C.P., Berwanger, O., *et al.*
647 (2020). Association Between Administration of Systemic Corticosteroids and Mortality Among
648 Critically Ill Patients With COVID-19: A Meta-analysis. JAMA *324*, 1330-1341.

649 Wajnberg, A., Amanat, F., Firpo, A., Altman, D.R., Bailey, M.J., Mansour, M., McMahon, M.,
650 Meade, P., Mendu, D.R., Muellers, K., *et al.* (2020). Robust neutralizing antibodies to SARS-
651 CoV-2 infection persist for months. Science *370*, 1227-1230.

652 Wang, P., Nair, M.S., Liu, L., Iketani, S., Luo, Y., Guo, Y., Wang, M., Yu, J., Zhang, B., Kwong,
653 P.D., *et al.* (2021a). Antibody resistance of SARS-CoV-2 variants B.1.351 and B.1.1.7. Nature.

654 Wang, S., Qiu, Z., Hou, Y., Deng, X., Xu, W., Zheng, T., Wu, P., Xie, S., Bian, W., Zhang, C., *et*
655 *al.* (2021b). AXL is a candidate receptor for SARS-CoV-2 that promotes infection of pulmonary
656 and bronchial epithelial cells. Cell Res *31*, 126-140.

657 Wang, Z., Schmidt, F., Weisblum, Y., Muecksch, F., Barnes, C.O., Finkin, S., Schaefer-Babajew,
658 D., Cipolla, M., Gaebler, C., Lieberman, J.A., *et al.* (2021c). mRNA vaccine-elicited antibodies
659 to SARS-CoV-2 and circulating variants. Nature *592*, 616-622.

660 Xie, X., Liu, Y., Liu, J., Zhang, X., Zou, J., Fontes-Garfias, C.R., Xia, H., Swanson, K.A., Cutler,
661 M., Cooper, D., *et al.* (2021). Neutralization of SARS-CoV-2 spike 69/70 deletion, E484K and
662 N501Y variants by BNT162b2 vaccine-elicited sera. Nat Med *27*, 620-621.

663 Zhou, D., Dejnirattisai, W., Supasa, P., Liu, C., Mentzer, A.J., Ginn, H.M., Zhao, Y.,
664 Duyvesteyn, H.M.E., Tuekprakhon, A., Nutalai, R., *et al.* (2021). Evidence of escape of SARS-
665 CoV-2 variant B.1.351 from natural and vaccine-induced sera. Cell.

666 Zhou, P., Yang, X.L., Wang, X.G., Hu, B., Zhang, L., Zhang, W., Si, H.R., Zhu, Y., Li, B.,
667 Huang, C.L., *et al.* (2020). A pneumonia outbreak associated with a new coronavirus of probable
668 bat origin. Nature *579*, 270-273.

669

670

671

672

673

674

675

676

677

678

679

680

681

682

683

684

685

686

687

688 **FIGURE LEGENDS**

689

690 **Figure 1. Schematic overview of the S protein from SARS-CoV-2 variant B.1.617**

691 The location of the mutations in the context of the B.1.617 S protein domain organization is
692 shown in the upper panel. RBD, receptor-binding domain; TD, transmembrane domain. The
693 location of the mutations in the context of the trimeric S protein is shown in the lower panels.
694 Color code: light blue, S1 subunit with RBD in dark blue; gray, S2 subunit; orange, S1/S2 and
695 S2' cleavage sites; red, mutated amino acid residues.

696

697 **Figure 2. The S protein of SARS-CoV-2 variant B.1.617 S drives efficient entry into human**
698 **cell lines**

699 (A) The S protein of the SARS-CoV-2 variant B.1.617 mediates robust entry into cell lines. The
700 indicated cell lines were inoculated with pseudotyped particles bearing the S proteins of the
701 indicated SARS-CoV-2 variants or wild-type (WT) SARS-CoV-2 S. Transduction efficiency was
702 quantified by measuring virus-encoded luciferase activity in cell lysates at 16-18 h post
703 transduction. Presented are the average (mean) data from three biological replicates (each
704 conducted with technical quadruplicates) for which transduction was normalized against SARS-
705 CoV-2 S WT (= 100%). Error bars indicate the standard error of the mean (SEM). Statistical
706 significance of differences between WT and variant S proteins was analyzed by one-way analysis
707 of variance (ANOVA) with Dunnett's posttest ($p > 0.05$, not significant [ns]; $p \leq 0.05$, *; $p \leq$
708 0.01, **; $p \leq 0.001$, ***). See also Figure S1.
709 (B) BHK-21 cells transfected with empty plasmid or ACE2 plasmid were inoculated with
710 pseudotyped particles bearing the indicated S proteins, VSV-G or no viral glycoprotein (control,
711 not shown). Presented are the average (mean) data from three biological replicates (each

conducted with technical quadruplicates) for which transduction was normalized against the background (signal obtained for particles without viral glycoprotein, = 1, indicated by the dashed line). Error bars indicate the SEM. Statistical significance of differences between empty vector and ACE2-transfected cells was analyzed by multiple t-test with correction multiple comparison (Holm-Sidak method; $p > 0.05$, ns; $p \leq 0.001$, ***).

Figure 3. Entry driven by the S protein of SARS-CoV-2 variant B.1.617 can be blocked with soluble ACE2 and Camostat mesylate

(A) S protein-bearing particles were incubated with different concentrations of soluble ACE2 (sol-ACE2) for 30 min at 37 °C, before the mixtures were inoculated onto Caco-2 cells.

(B) Caco-2 target cells were pre-incubated with different concentrations of the serine protease inhibitor Camostat mesylate for 1 h at 37 °C, before S protein-bearing particles were added.

All panels: Transduction efficiency was quantified by measuring virus-encoded luciferase activity in cell lysates at 16-18 h post-transduction. For normalization, SARS-CoV-2 S protein-driven entry in the absence of sol-ACE2 or Camostat was set as 0% inhibition. Presented are the average (mean) data from three biological replicates (each performed with technical quadruplicates. Error bars indicate the SEM. Statistical significance of differences between WT and variant S proteins or VSV-G was analyzed by two-way ANOVA with Dunnett's posttest ($p > 0.05$, ns [not indicated]; $p \leq 0.001$, ***).

Figure 4. The S protein of SARS-CoV-2 variant B.1.617 is resistant to neutralization by Bamlanivimab

S protein-bearing particles were incubated with different concentrations of monoclonal antibodies for 30 min at 37 °C before the mixtures were inoculated onto Vero cells. Transduction efficiency

was quantified by measuring virus-encoded luciferase activity in cell lysates at 16-18 h post-transduction. For normalization, SARS-CoV-2 S protein-driven entry in the absence of monoclonal antibody was set as 0% inhibition. Presented are the average (mean) data from three biological replicates (each performed with technical quadruplicates). Error bars indicate the SEM. Statistical significance of differences between WT and variant S proteins was analyzed by two-way ANOVA with Dunnett's posttest ($p > 0.05$, ns [not indicated]; $p \leq 0.05$, *; $p \leq 0.01$, **; $p \leq 0.001$, ***). See also Figure S2.

Figure 5. The S protein of SARS-CoV-2 variant B.1.617 evades neutralization by antibodies induced upon infection or vaccination with BNT162b2

The S protein of SARS-CoV-2 variant B.1.617 evades neutralization by convalescent plasma (A) or plasma from BNT162b2-vaccinated individuals (B).

Both panels: S protein-bearing particles were incubated with different plasma dilutions (derived from infected or vaccinated individuals) for 30 min at 37 °C before the mixtures were inoculated onto Vero cells. Transduction efficiency was quantified by measuring virus-encoded luciferase activity in cell lysates at 16-18 h post-transduction and used to calculate the plasma/serum dilution factor that leads to 50 % reduction in S protein-driven cell entry (neutralizing titer 50, NT50). Presented are the average (mean) data from a single biological replicate (performed with technical quadruplicates). Error bars indicate the standard deviation. Identical plasma samples are connected with lines and the numbers in brackets indicate the average (mean) reduction in neutralization sensitivity for the S proteins of the respective SARS-CoV-2 variants. Statistical significance of differences between WT and variant S proteins was analyzed by paired two-tailed Students t-test ($p > 0.05$, ns; $p \leq 0.01$, **; $p \leq 0.001$, ***). See also Figure S3.

Figure 1

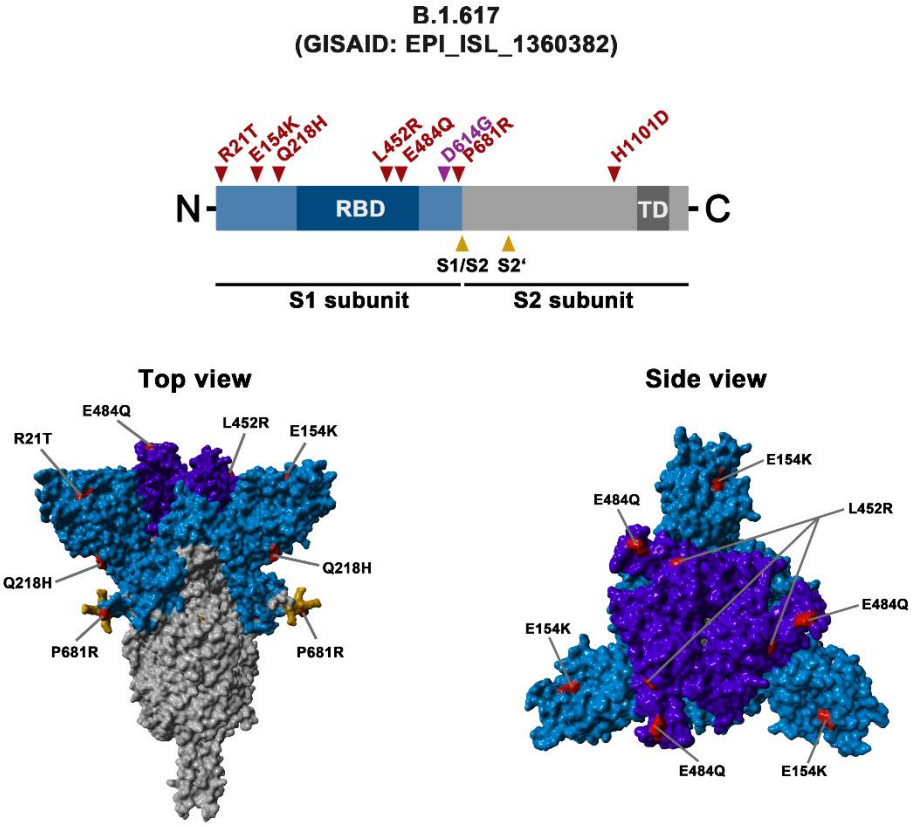

760

Figure 2

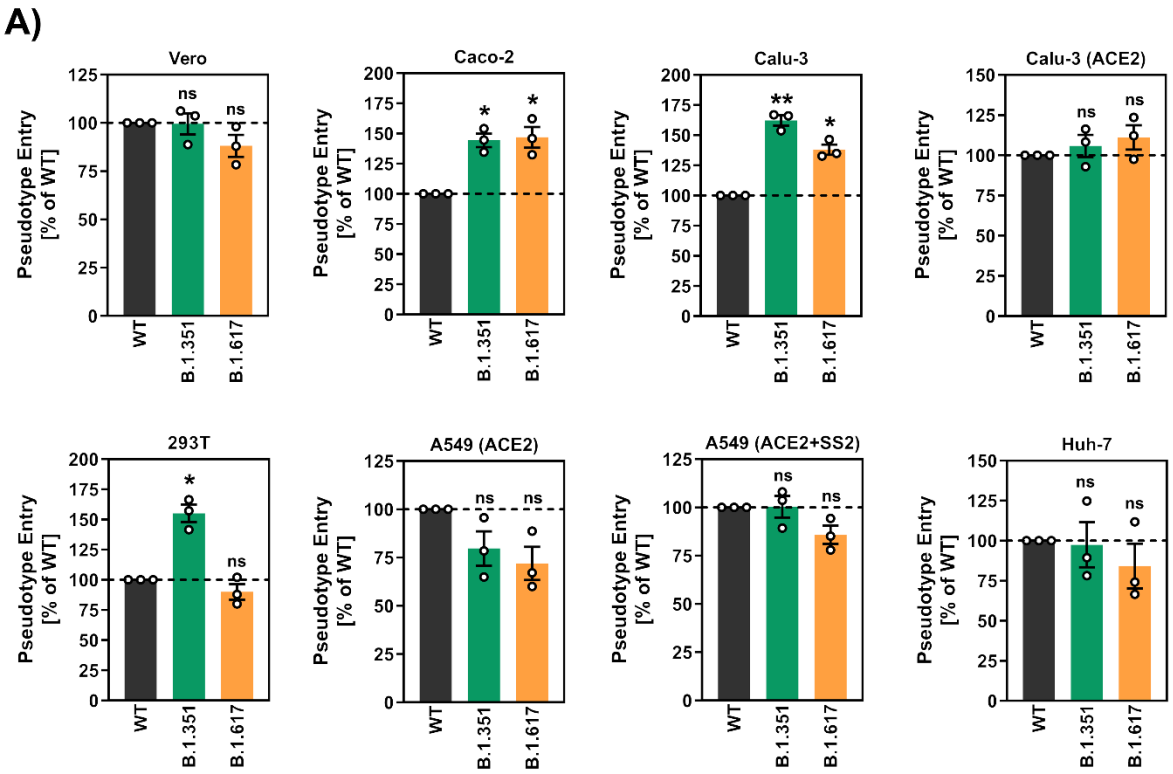

761

Figure 3

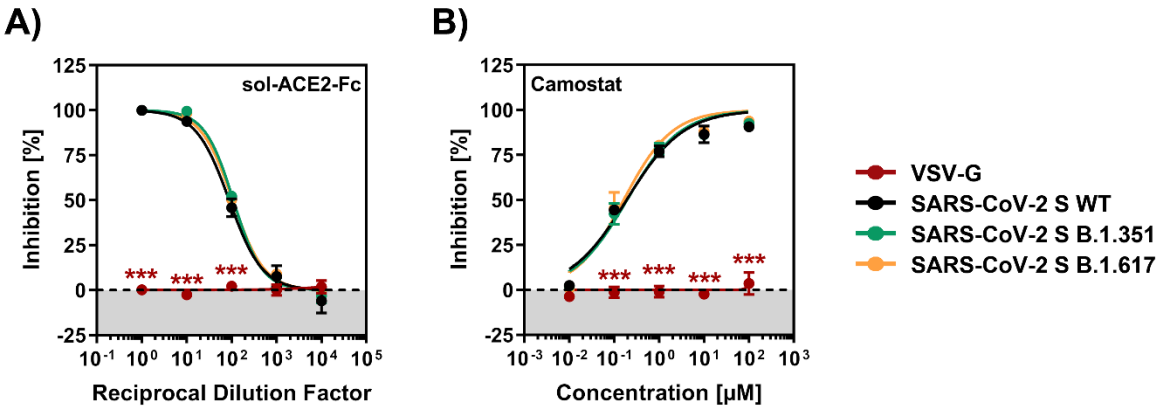

762

Figure 4

A)

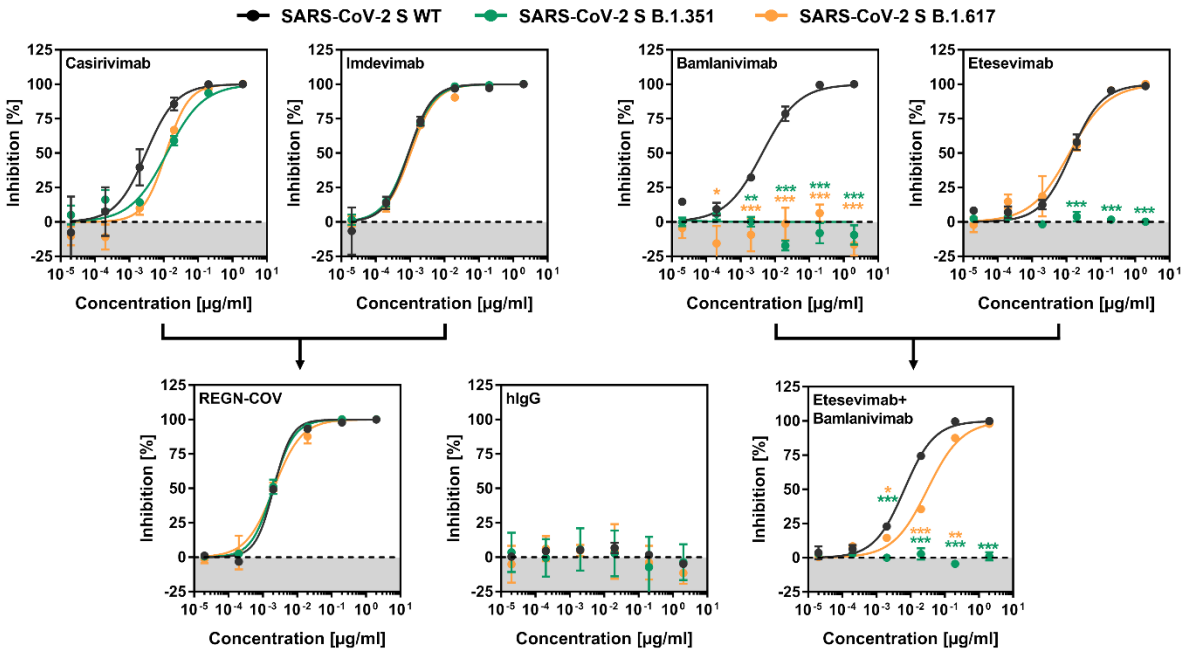

763

Figure 5

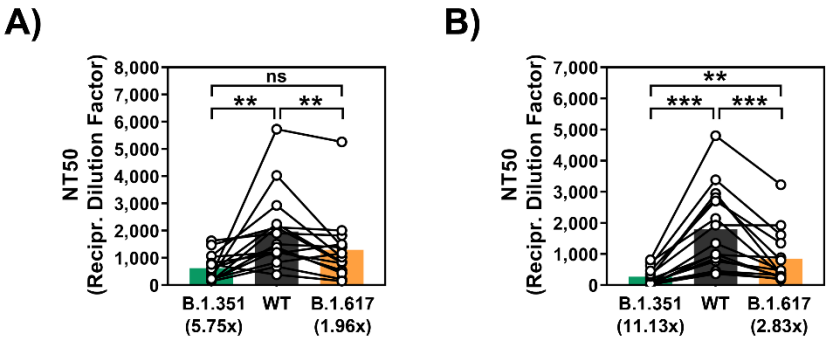

764

765 # SUPPLEMENTAL INFORMATION

Figure S1

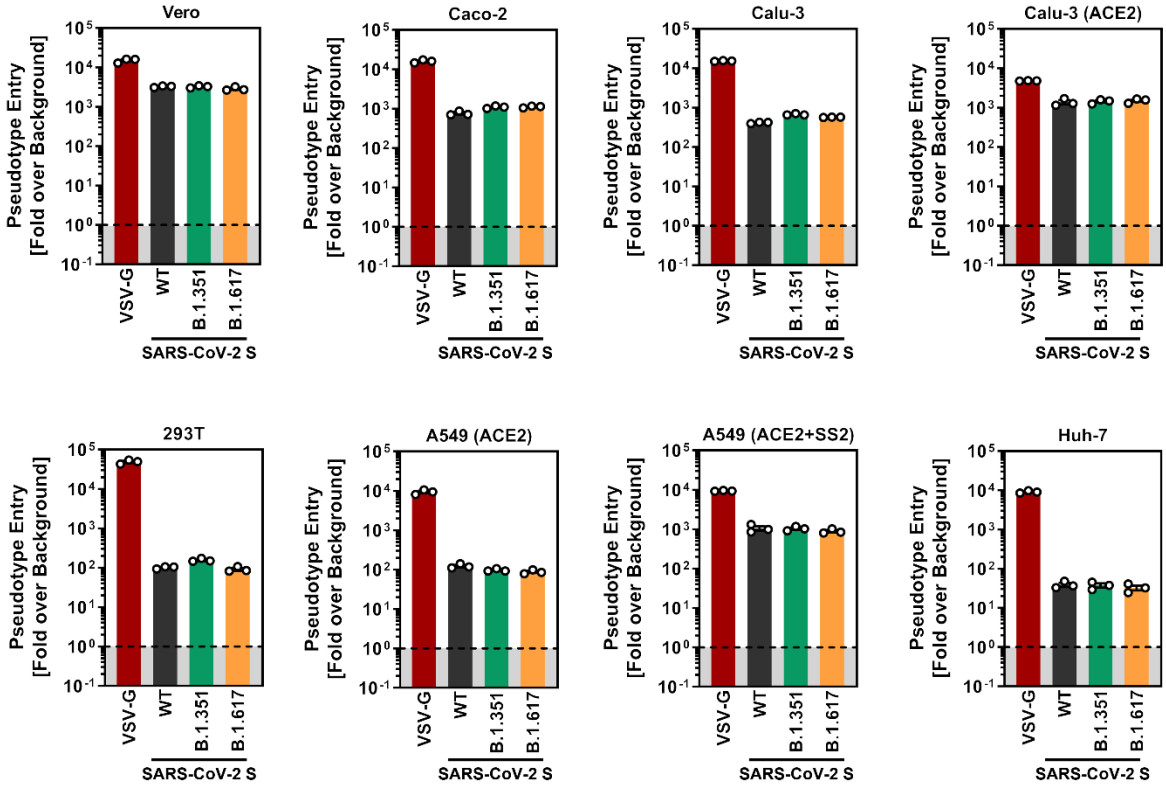

Figure S1. Transduction data normalized against the assay background (related to Figure 2). The experiment was performed as described in the legend of Figure 1A. Presented are the average (mean) data from the same three biological replicates (each conducted with technical quadruplicates) as presented in Figure 1A with the difference that this time transduction was normalized against signals obtained from cells inoculated with particles bearing no viral glycoprotein (background, set as 1). Further, transduction data of particles bearing VSV-G are included. Error bars indicate the SEM.

Figure S2

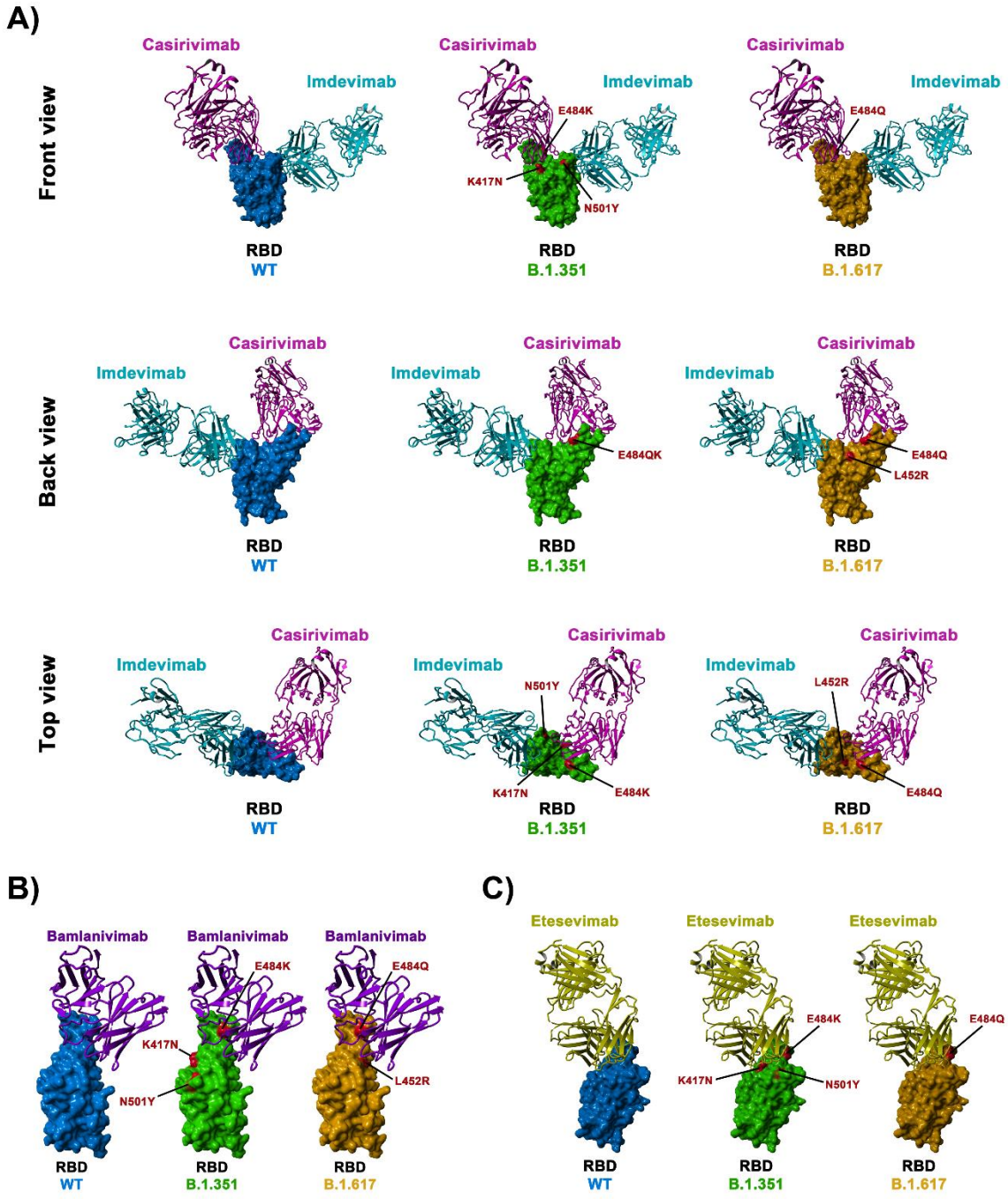

Fígure S2. Location of SARS-2-S B.1.351 and B.1.617 RBD mutations with respect to the binding interface of Casirivimab and Imdevimab (A), Bamlanivimab (B) and Esetevimab (C) (related to Figure 4).

780 The protein models of the SARS-2-S receptor-binding domain (RBD, blue) in complex with
781 antibodies Casirivimab (pink) and Imdevimab (turquoise) were constructed based on the 6XDG
782 template (Hansen et al., 2020), while the protein models of the SARS-2-S RBD in complex with
783 antibody Bamlanivimab (purple) and Etesevimab (yellow) were based on the PDB: 7L3N (Jones
784 et al., 2020) and PDB: 7C01 (Shi et al., 2020) template, respectively. Residues highlighted in red
785 indicate amino acid variations found in the SARS-CoV-2 variants.

Figure S3

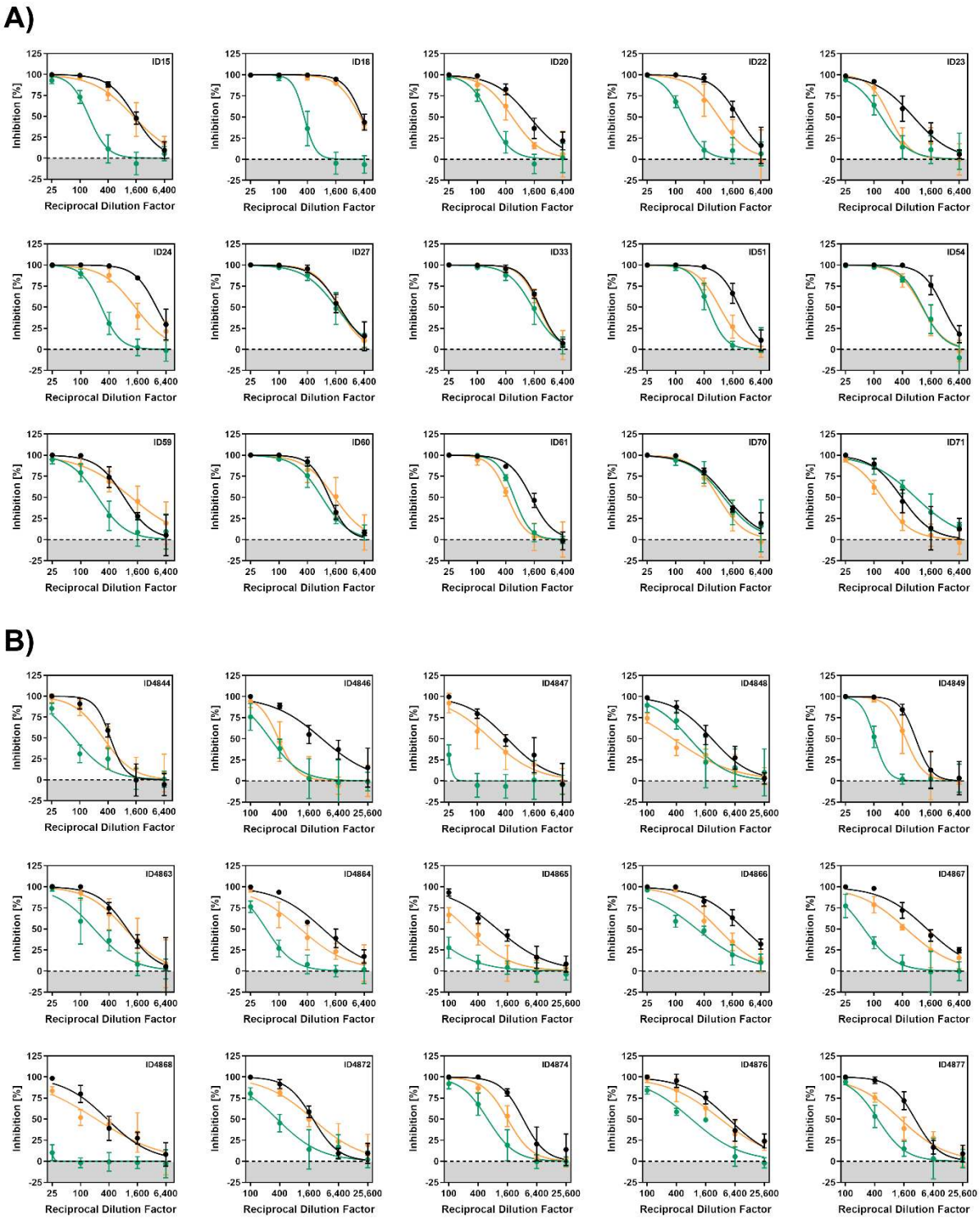

Figure S3. Individual neutralization data (related to Figure 5).

789 Pseudotypes bearing the indicated S proteins were incubated (30 min, 37 °C) with different
790 dilutions of plasma derived from COVID-19 patients (A) or individuals vaccinated with the
791 Pfizer/BioNTech vaccine Comirnaty/BNT162b2 (B) and inoculated onto Vero target cells.
792 Transduction efficiency was quantified by measuring virus-encoded luciferase activity in cell
793 lysates at 16-18 h posttransduction. Presented are the data from a single representative experiment
794 conducted with technical Quadruplicates. For normalization, inhibition of S protein-driven entry
795 in samples without plasma was set as 0 %. Error bars indicate the SD. The data were further used
796 to calculated the plasma/serum dilution that leads to 50% reduction in S protein-driven cell entry
797 (neutralizing titer, NT50, shown in Figure 5).

Table S1

Table S1: COVID-19 patient data

			WHO classification upon ICU admission															
ID	**Symptoms before hospital admission (days)**	**Symptoms before ICU admission (days)**	**mild**	**moderate**	**severe**	**critical**	**Age**	**Sex**	**Diabetes**	**Hypertension**	**Cardiac disease**	**Chronic lung disease + Asthma**	**Cerebrovascular disease**	**Chronic kidney disease**	**Immunosuppression**	**Cancer**	**Obesity**	**Smoking**
SI 15	ND	ND	-	-	-	x	65	M			x					x		
SI 16	ND	ND	-	x	-	x	71	M								x		
SI 18	2	11	-	-	-	x	74	F	x	x						x		
SI 20	ND	ND	-	-	-	x	61	M	x			x						
SI 22	5	5	-	-	-	x	25	F									x	
SI 23	2	8	-	-	x	-	69	F	x									
SI 24	4	8	-	-	-	x	61	M		x								x
SI 27	ND	ND	-	-	-	x	52	M	x	x								
SI 33	1	14	-	-	-	x	75	M	x	x	x							
SI 51	4	12	-	-	-	x	71	M										
SI 54	8	7	-	-	-	x	58	F		x		x				x		
SI 59	6	3	-	-	-	x	46	M		x	x			x				x
SI 60	5	6	-	-	-	x	61	F				x						
SI 61	7	2	-	-	-	x	50	M				x					x	
SI 70	ND	ND	-	-	x	-	34	F										
SI 71	5	3	-	x	-	-	54	M		x								

ND =Not determined

Table S2

Table S2. BNT162b2-vaccinated patient data.

BNT162b2-vaccinated patient data. Serological data shows antibody titer against spike (IgG) protein determined by quantitative ELISA (SARS-CoV-2-QuantiVac; Euroimmun, Lübeck, Germany) according to the manufacturer's instructions. Antibody levels are expressed as RU/ml assessed from a calibration curve with values above 10 RU/mL defined as positive, values beyond the standard curve are expressed as >120 RU/ml.

ID	Age (y)	Gender	Time since 2nd vaccination (d)	Spike-IgG
4844	47	f	31	>120
4846	28	f	29	>120
4847	57	f	26	>120
4848	29	m	26	>120
4849	39	m	24	>120
4863	58	f	26	>120
4864	53	f	26	>120
4865	57	m	25	>120
4866	59	f	29	>120
4867	52	f	30	34,4
4868	56	f	30	119.6
4872	37	f	25	>120
4874	26	f	29	>120
4876	27	f	30	>120
4877	29	f	28	>120